JOC The Journal of Organic Chemistry

Article

pubs.acs.org/joc

Study of a Two-Stage Photobase Generator for Photolithography in Microelectronics

Nicholas J. Turro,*[,†] Yongjun Li,[†] Steffen Jockusch,[†] Yuji Hagiwara,[‡] Masahiro Okazaki,[‡] Ryan A. Mesch,[‡] David I. Schuster,[§] and C. Grant Willson*[,‡]

[†]Department of Chemistry, Columbia University, New York, New York 10027, United States

[‡]Chemistry Department, University of Texas, Austin, Texas 78741, United States

[§]Department of Chemistry, New York University, New York, New York 10003, United States

Supporting Information

ABSTRACT: The investigation of the photochemistry of a two-stage photobase generator (PBG) is described. Absorption of a photon by a latent PBG (**1**) (first step) produces a PBG (**2**). Irradiation of **2** in the presence of water produces a base (second step). This two-photon sequence (**1** + $h\nu$ → **2** + $h\nu$ → base) is an important component in the design of photoresists for pitch division technology, a method that doubles the resolution of projection photolithography for the production of microelectronic chips. In the present system, the excitation of **1** results in a Norrish type II intramolecular hydrogen abstraction to generate a 1,4-biradiacal that undergoes cleavage to form **2** and acetophenone ($\Phi \sim 0.04$). In the second step, excitation of **2** causes cleavage of the oxime ester ($\Phi = 0.56$) followed by base generation after reaction with water.

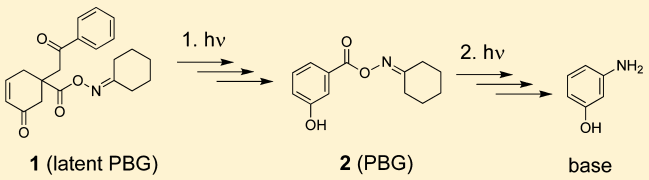

INTRODUCTION

The main method for increasing computational speed in modern computers is the reduction of the size of the electronic features on the processor chip. Several techniques have been proposed to achieve higher resolution in optical lithography for microelectronic chip manufacturing.[1] A new technique, called pitch division technology, has demonstrated doubling of the resolution in the projection printing process using conventional photolithography tools without additional processing steps.[2] In conventional photolithography, a photoacid generator (PAG) is used, which upon light exposure generates acid that catalyzes a deprotection reaction which in turn modifies the solubility of the resist polymer. In the new pitch division technology, a combination of a PAG and a photobase generator (PBG) is used. By carefully matching the kinetics and stoichiometry of the photoreactions, the generated base can neutralize the acid at areas of highest UV light exposure, which leaves highly exposed areas and the unexposed areas undesolved during resist development. In areas of weaker light exposure, not enough base is produced to neutralize the generated acid, and therefore, the resist polymer is dissolved in these weakly exposed areas in the development step. This leads to a division of the pitch and doubling of the resolution.[2,3] However, line edge roughness of the developed resist features prevents commercial implementation of pitch division.[3] It has been proposed that the line edge roughness can be improved by creating a delay in the onset of base generation. One method to achieve this delayed base generation is through the use of a two-stage PBG,[3,4] one that requires two sequential photolysis steps to produce a molecule of base (eq 1). In the first photochemical step, a latent PBG (**A**) produces

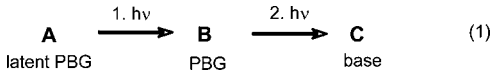

(1)

an intermediate species that is an active PBG (**B**), which in a second photochemical step produces a base (**C**). Here we report the study of a proof-of-principle system that demonstrates the feasibility of this two-stage PBG proposal.

Our design of such a system is shown in Scheme 1.[4] The first photochemical step is an example of a Norrish type II reaction,[5] which involves intramolecular hydrogen atom abstraction by a ketone to form a 1,4-biradical (1,4-BR) (reaction a, Scheme 1). The 1,4-biradical has several possible reaction pathways that lead to stable products: cleavage of the 2,3 bond to produce a 2,4-cyclohexadienone and an enol (reaction b) that tautomerize to PBG (**2**) (reaction c) and acetophenone (**3**) (reaction d). Formation of a cyclobutanol (not shown) by intramolecular radical recombination of the 1,4-BR could occur as a side reaction. The second photochemical step involves cleavage of the N−O single bond of **2** to produce a radical pair (primary RP) (reaction e, Scheme 1), which then undergoes decarboxylation to form a secondary radical pair (secondary RP) (reaction f) followed by radical pair recombination to produce the imine **4** (reaction g).[6,7] The imine, already a weak base, can undergo hydrolysis during the resist development to generate the stronger base 3-aminophenol (**5**) (reaction h).

Special Issue: Howard Zimmerman Memorial Issue

Received: September 30, 2012
Published: October 29, 2012

   dx.doi.org/10.1021/jo302149u | J. Org. Chem. 2013, 78, 1735−1741

Scheme 1. Overall Pathway for Sequential Photolysis of 1 (Latent PBG) and 2 (PBG) to Form Base 5

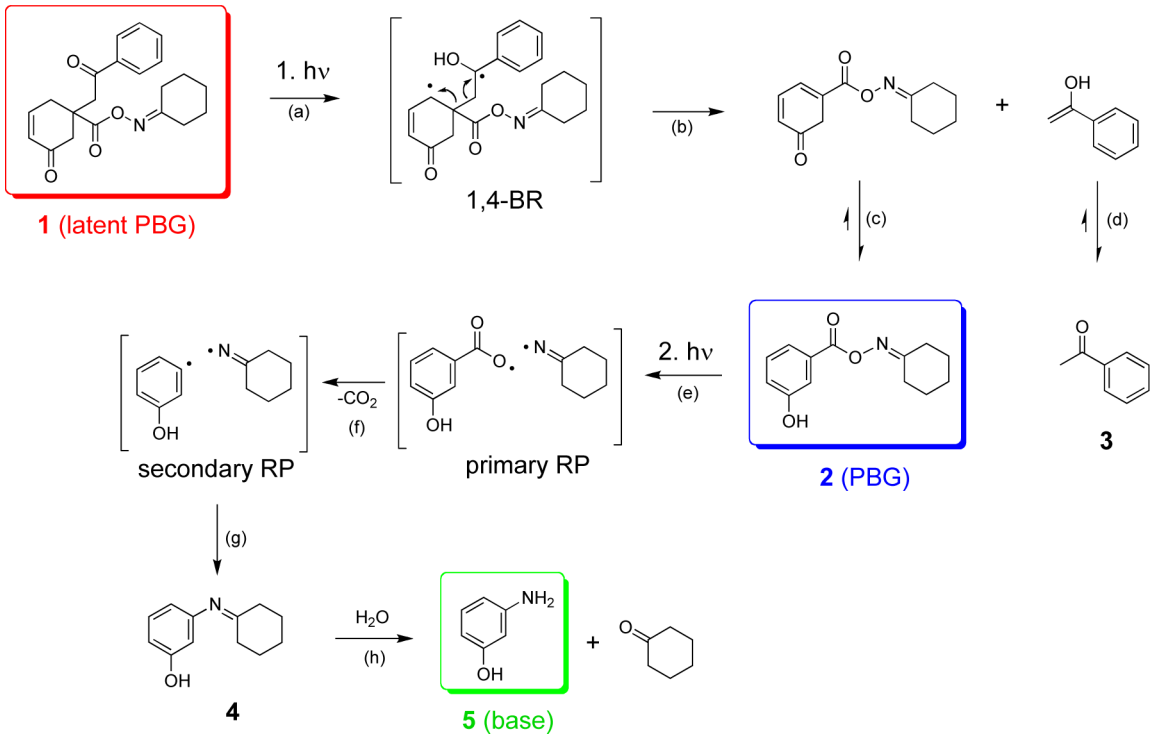

RESULTS AND DISCUSSION

The mechanism of photochemical formation of **2** from **1** deserves some detailed attention since **1** possesses two potentially active chromophores, an acetophenone (AP) moiety and a cyclohexenone (CH) moiety, each possessing its own unique photochemistry. Figure 1 shows absorption spectra of **1**, acetophenone **3**, and a model compound **6** which does not contain the acetophenone chromophore. For our photochemical experiments, we selected two different excitation wavelength, 254 and 300 nm. The acetophenone chromophore absorbs strongly at 254 nm (ε^3 = 2780 M^{-1} cm^{-1}), whereas the cyclohexenone-containing model compound (**6**) shows only weak absorption (ε^6 = 41 M^{-1} cm^{-1}). This ensures predominant light absorption at 254 nm by the acetophenone chromophore in **1**. We also looked at 300 nm excitation because cleaner photoreactions with less side reactions are often observed at longer wavelengths. However, the cyclohexenone (CH) chromophore shows significant absorption at 300 nm (ε^6 = 22 M^{-1} cm^{-1}) vis-a-vis the acetophenone chromophore (ε^3 = 54 M^{-1} cm^{-1}), which would lead to less efficient photoconversion.

The state energy diagram for these chromophores is shown in Figure 2. The singlet and triplet energies ($^{AP}E_{S1}$ = 80 kcal mol^{-1} and $^{AP}E_{T1}$ = 74 kcal mol^{-1})[8] of the acetophenone (AP) moiety are higher than those of the cyclohexenone (CH) moiety ($^{CH}E_{S1}$ = 75 kcal mol^{-1} and $^{CH}E_{T1}$ = 63 kcal mol^{-1}).[9] Therefore, singlet and triplet energy transfer from excited states of the AP to CH moiety is energetically favorable. From the state energy diagram, photoexcitation of the acetophenone moiety generates $^{AP}S_1$, which could undergo intersystem crossing to $^{AP}T_1$ or energy transfer to CH. If the $^{CH}S_1$ state is populated, it can undergo intersystem crossing to $^{CH}T_1$ or radiationless deactivation to $^{CH}S_0$. In order for the type II process to occur with substantial quantum efficiency, the yield of $^{AP}T_1$ must be high and the rate constant of the type II reaction from $^{AP}T_1$ must be competitive with the rate constant for energy transfer from $^{AP}T_1$ to $^{CH}T_1$. These possibilities are considered quantitatively in the next section using data available in the literature.

Intramolecular triplet−triplet energy transfer has been investigated for the bichromophoric donor−acceptor systems D−$(CH_2)_n$-O−A (D = benzoyl, A = 2-naphthyl) where n = 3−14.[10] The values of E_T for the benzoyl and naphthyl groups are ∼73 and 62 kcal mol^{-1}, respectively. Therefore, intramolecular triplet−triplet energy transfer is strongly exothermic. The highest energy transfer rate constant has been observed for the shortest linker (n = 3; k_{ET} = 1.6 × 10^9 s^{-1}).[10] This rate constant serves us as an estimate of the triplet energy transfer rate constant from the AP moiety to the CH moiety in **1**. Since energy transfer occurs by the exchange mechanism for both S_1 and T_1, we can assume k_{ET} ∼ 2 × 10^9 s^{-1} is the rate constant for energy transfer from either S_1 or T_1 of AP to CH.

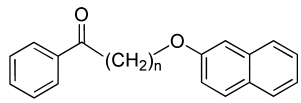

To simplify our experimental studies on the phototransformation from **1** to **2**, we synthesized a model compound (**1M**, Scheme 2) which does not contain the oxime ester moiety. Scheme 2 shows the rate constants for the competing processes leading from $^{AP}S_1$ to the triplet 1,4-BR produced by type II hydrogen abstraction, based on data from the literature. Starting from $^{AP}S_1$, the rate constant of intersystem crossing to $^{AP}T_1$ (k_{isc} = 4 × 10^{10} s^{-1})[11] is estimated to be about 10 times faster than the rate constant of energy transfer from $^{AP}S_1$ to $^{CH}S_1$. Therefore, it is expected that the acetophenone $^{AP}T_1$ is the starting point of the photochemistry after photoexcitation of **1M**. In this analysis, we assume that only triplet type II reaction and triplet−triplet energy transfer provide the major deactivation processes on the pathway to reaction products. The rate constant for type II (k_H) is assumed to be faster than that for the valerophenone system (k_H = 1.3 × 10^8 s^{-1})[5] since

dx.doi.org/10.1021/jo302149u | J. Org. Chem. 2013, 78, 1735−1741

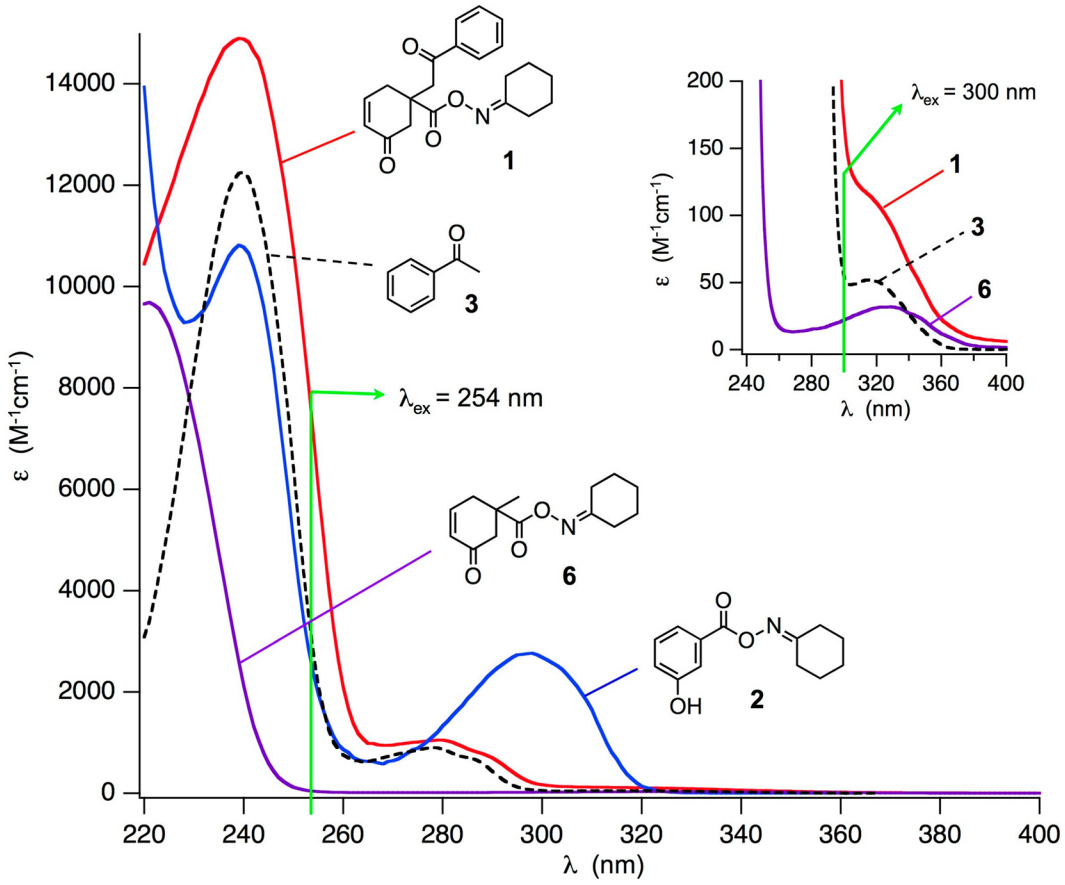

Figure 1. Absorbance of **1**, **2**, **3**, and model compound **6** lacking the acetophenone chromophore in acetonitrile solutions.

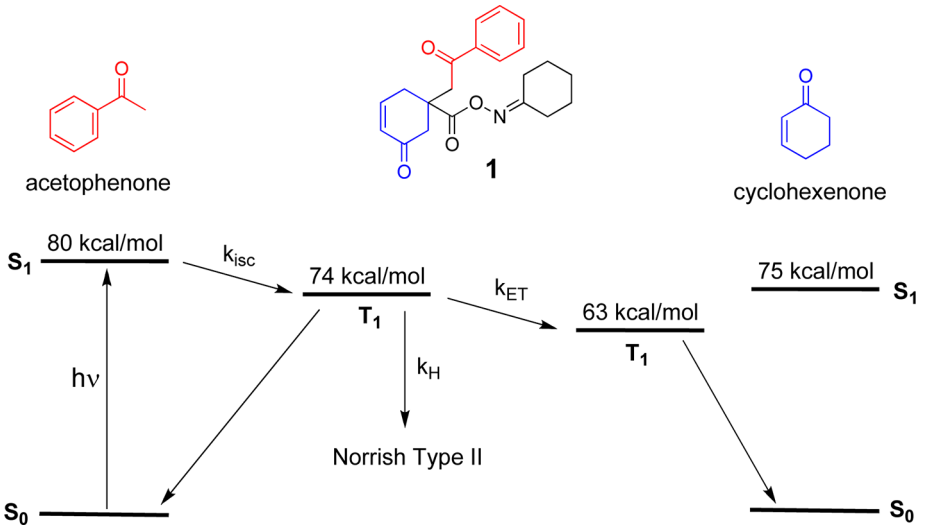

Figure 2. Energy diagram of acetophenone and cyclohexenone, the two chromophores of **1**.

this process for **1M** involves the abstraction of an *activated* allylic H. From the literature, the rate constant k_H of ~5 × 10^8 s^{-1} is representative for abstraction of an allylic H.[5] From the D−$(CH_2)_n$O−A systems for n = 3−14, a value of k_{ET} ~ 2 × 10^9 s^{-1} is selected as the maximum value of k_{ET} for intramolecular triplet−triplet energy transfer for a flexible chain. Under these assumptions, the ratio of the competitive rate constants k_H and k_{ET} is ~0.5 × 10^9 s^{-1}/~2 × 10^9 s^{-1} = 0.25, and the maximum quantum yield of formation of **3** (Φ_3) could be as high as 0.25, a significant value. The experimental value of Φ_3 will be lower if k_H has been overestimated or if k_{ET} is underestimated or if the conversion of the 1,4-biradical to the final products is inefficient.

Laser flash photolysis experiments were performed to verify that triplet states of the acetophenone moiety in **1M** are efficiently quenched by energy transfer to the cyclohexenone moiety and/or Norrish type II reaction. Pulsed laser excitation at 266 nm of acetophenone (**3**) in deoxygenated acetonitrile showed the typical triplet−triplet absorption with maximum at 320 nm and a

dx.doi.org/10.1021/jo302149u | J. Org. Chem. 2013, 78, 1735−1741

Scheme 2. Estimated Rate Constants for the Photoconversion of 1M to 3 and 7

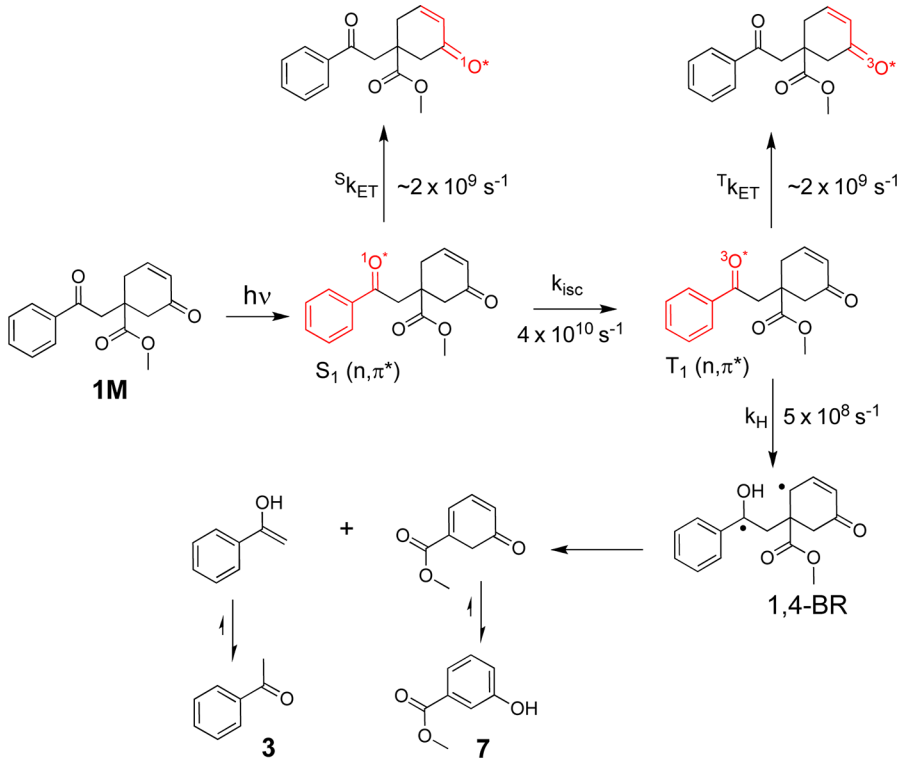

lifetime of ~18 μs under our experimental conditions (for details, see Supporting Information, Figure S1, blue line).[12] Solutions of **1M** under the same experimental conditions (the same absorbance at 266 nm and the same laser power) did not show any significant triplet−triplet absorption with the time resolution limited by our experimental setup (Supporting Information, Figure S1, red line), which suggests that the triplet lifetime of **1M** is shorter than 10 ns at room temperature.

Low-temperature phosphorescence experiments were performed in an ethanol matrix at 77 K to investigate if the triplet states of the AP moiety of **1M** are detectable by its phosphorescence. Excitation of AP (**3**) in an ethanol matrix at 77 K with light of 315 nm showed the typical phosphorescence spectrum (Supporting Information, Figure S2, blue line). However, only a small broad luminescence signal (<5% compared to **3**) was observed from **1M** (Figure S2, red line) under the same experimental conditions (same absorbance at 315 nm). The absence of phosphorescence from the AP moiety in **1M** is an indication of efficient triplet quenching, even in a rigid matrix at 77 K. Because an activation energy is associated with Norrish type II H-abstractions, the process is typically not observed at 77 K;[13] thus triplet quenching by energy transfer to CH is probably occurring.

Steady-state photolysis experiments in deoxygenated acetonitrile solutions were conducted to see if the predicted products **3** and **7** are formed upon photolysis of **1M** at 300 nm. Figure 3 shows the HPLC analysis of these irradiated solutions. Two new peaks with retention times of 3.5 and 4.8 min appeared and were assigned to the predicted photoproducts **7** and **3**, respectively, based on co-injection with authentic samples (Supporting Information, Figure S3). Considering the extinction coefficients of the three compounds (**1M**, **3**, and **7**) at 288 nm, the analyzing wavelength used in these HPLC experiments, molar equivalents of both products (**3** and **7**) are formed for every lost molecule of starting material (**1M**). This is an indication of a clean photoprocess with negligible side reactions. Photolysis experiments were also performed at 254 nm. However, more side products were observed according to HPLC analysis (Supporting Information, Figure S5).

The quantum yield of the photoconversion of **1M** to **3** and **7** was determined using valerophenone as actinometer. Valerophenone shows similar absorption properties to **1M** and undergoes efficient Norrish type II reaction upon photolysis with a quantum yield of Φ = 1.0 (loss of valerophenone) in acetonitrile.[14] Using valerophenone as actinometer (for full details, see the Supporting Information), a quantum yield of Φ_3 = 0.04 ± 0.01 for the production of **3** from **1M** was determined at 254 nm. A smaller quantum yield, Φ_3 = 0.02 ± 0.01, was observed for photolysis at 300 nm because of competing light absorption by the cyclohexenone chromophore (see Figure 1). The experimental quantum yields are lower than those estimated from the literature values of k_{ET} and k_H (Scheme 2). Thus, we conclude that there are either competing or unaccounted deactivation pathways or inaccurate estimations of the values of k_{ET} and k_H.

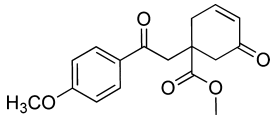

p-CH_3O-**1M**

The rate constant for type II reactions in valerophenone is known to be affected by substitution at the phenyl ring.[15] A *p*-OCH_3 substituent changes the nature of the lowest triplet state from a nπ^* (unsubstituted valerophenone) to a $\pi\pi^*$ state. Type II reactions are typically not observed from $\pi\pi^*$ states.[15] A *p*-OCH_3-substituted derivative of **1M** (*p*-OCH_3-**1M**) should show negligible type II reaction (k_H) because of its $\pi\pi^*$ triplet state. However, energy transfer from the *p*-OCH_3 acetophenone moiety to the cyclohexenone moiety (k_{ET}) should not be significantly affected by the *p*-OCH_3 substituent. Laser flash photolysis

dx.doi.org/10.1021/jo302149u | J. Org. Chem. 2013, 78, 1735−1741

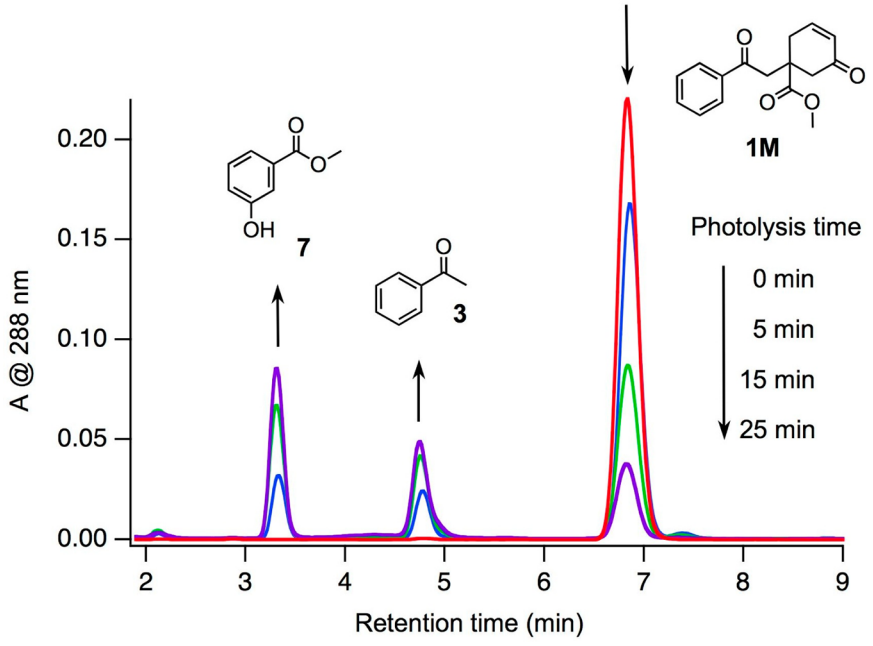

Figure 3. HPLC analysis of irradiation at 300 nm of **1M** in deoxygenated acetonitrile solutions. Analyte detection by UV spectroscopy at 288 nm.

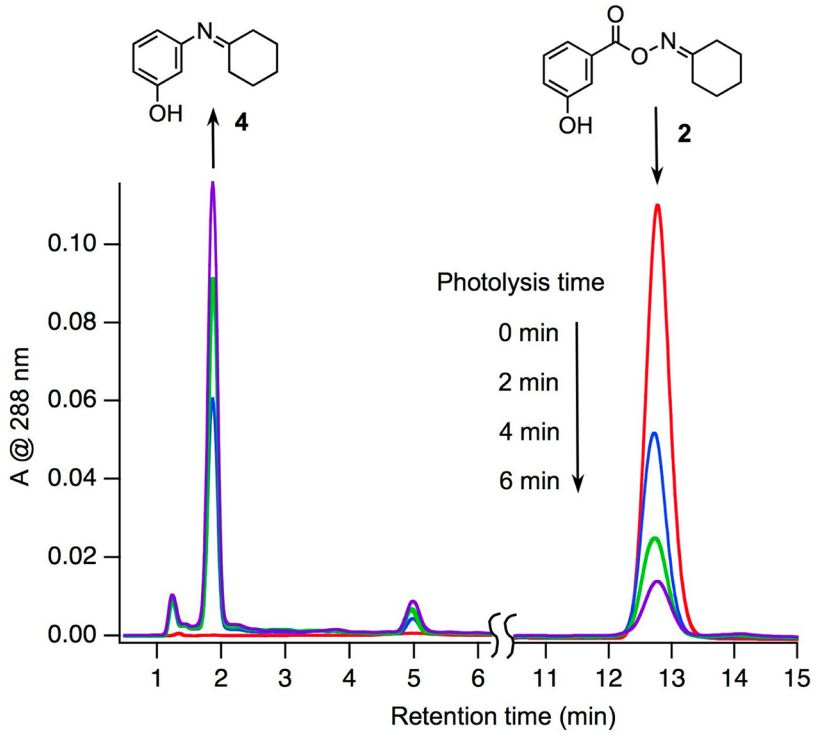

Figure 4. HPLC analysis of photolysis at 254 nm of **2** in deoxygenated acetonitrile solutions. Analyte detection by UV spectroscopy at 288 nm. See Supporting Information, Figure S8, for full HPLC traces.

at room temperature (Figure S6, Supporting Information) and low-temperature phosphorescence experiments (Figure S7) show efficient triplet quenching of *p*-OCH_3-**1M** by the CH moiety. Steady-state photolysis and HPLC analysis showed only negligible amounts of photoproducts. A low quantum yield of *p*-OCH_3-**1M** loss of $\Phi = 0.002 \pm 0.001$ was determined by HPLC analysis. Therefore, photolysis experiments with *p*-OCH_3-**1M** verify that our proposed reaction mechanism generates the observed photoproducts (**2** and **3**) through type II reactions from triplet excited states of the AP moiety (Scheme 2) and not through reactions of triplet excited states of the CH moiety.

To study the efficiency of the second photolysis step, the generation of the base precursor **4** from **2** (Scheme 1, reactions e−g), deoxygenated acetonitrile solutions of **2** were irradiated at 254 nm and analyzed by HPLC. Figure 4 shows HPLC traces after different photolysis times. The peak at 12.8 min (assigned to **2**) decreased with increasing photolysis time, while the major product peak at 1.9 min increased. This new peak was assigned to

dx.doi.org/10.1021/jo302149u | *J. Org. Chem.* 2013, 78, 1735−1741

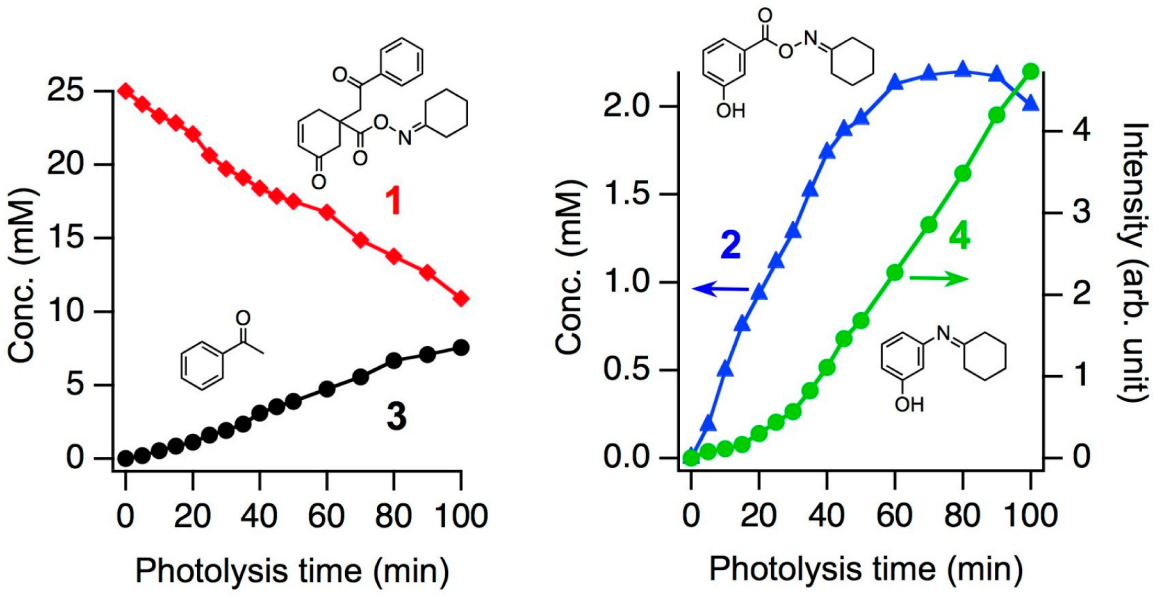

Figure 5. Kinetics of photoconversion of **1** (25 mM) to **2**, **3**, and **4** determined by HPLC analysis of photolyzed acetonitrile solutions a 254 nm. See Supporting Information, Figure S11, for HPLC traces.

the expected photoproduct **4** based on HPLC-MS analysis (Supporting Information, Figures S9 and S10). A quantum yield for loss of **2** of $\Phi = 0.56 \pm 0.02$ was determined using valerophenone as actinometer, which demonstrates the efficiency of this photoreaction.

Using the model compounds **1M** and **2**, both photochemical steps have been investigated separately as described above. To study the entire sequential two-step base generation as outlined in Scheme 1, acetonitrile solutions of **1** were irradiated at 254 nm and analyzed by HPLC (Supporting Information, Figure S11). Using authentic samples and quantitative HPLC calibration, the concentrations of the major product (**3**) and intermediate (**2**) were determined. Figure 5 shows the concentrations of **1**, **2**, and **3** with increasing photolysis time. With consumption of **1**, the concentrations of **2** and **3** increase. As soon as enough **2** is generated to compete for the excitation light at 254 nm (ε^2 = 2360 M^{-1} cm^{-1} and ε^1 = 7070 M^{-1} cm^{-1}; Figure 1), photoproduct **4** is formed and the concentration of **2** decreases. We were unable to determine the concentrations for the generation of **4** due to the lack of an authentic sample of **4** for quantitative HPLC calibration. Therefore, only relative concentrations of **4** are plotted in Figure 5 (right, green line). The formation of significant amounts of **4** is observed after an inhibition time of ~20 min (Figure 5, green line), which shows that only at higher light doses the second photolysis step gains importance. This delayed base generation is a desired characteristic for potential application of **1** in photoresist systems using pitch division technology.[3]

CONCLUSIONS

We have demonstrated that **1**, a latent PBG, functions as a two-stage PBG. Upon photolysis of **1**, the generated triplet excited states of the acetophenone moiety undergo Norrish type II reaction with the CH moiety, leading to generation of **2** (PBG). The quantum yield of this type II reaction of the AP triplet is relatively low ($\Phi \sim 0.04$ at $\lambda_{ex} = 254$ nm) due to competition with the more efficient triplet energy transfer from the acetophenone to the cyclohexenone moiety. However, this low quantum yield for type II reaction is sufficient to generate significant amounts of **2** on steady-state irradiation. In the second photolysis step, the oxime ester **2** (PBG) undergoes N−O cleavage with a high quantum yield ($\Phi = 0.56$ for direct photolysis of **2**, $\lambda_{ex} = 254$ nm) leading to the imine **4**, which generates the desired base upon reaction with water. Because the production of **4** from **1** involves two sequential photolysis steps, the desired delayed generation of **4** was observed. However, for the material to be used in practical resist formulations for photolithography with 193 nm light, the relative rates of both sequential steps should be of similar magnitude. The rates are determined by the extinction coefficients of **1** and **2** at the excitation wavelength and the quantum yields for each photoreaction step. While the extinction coefficients of **1** and **2** are similar, the quantum yield for the second step (**2** + $h\nu \rightarrow$ base) is 1 order of magnitude larger compared to the first step (**1** + $h\nu \rightarrow$ **2**). Therefore, the overall rate is dominated by the kinetics of the slowest step (**1** + $h\nu \rightarrow$ **2**), and the desired delay in the onset of base generation is reduced. Further chemical modification of the system is needed before it meets the requirements for industrial use in resist formulations for pitch division photolithography.

EXPERIMENTAL SECTION

Materials. The synthesis and characterization of compounds **1**, **2**, **6**, **1M**, and *p*-OCH_3-**1M** have been described previously.[4]

Laser flash photolysis experiments employed the pulses from a Nd:YAG laser (266 nm, 5 ns) and a computer-controlled system, which has been described previously.[16] Acetonitrile solutions containing **1M**, **3**, *p*-OCH_3-**1M**, or *p*-OCH_3-acetophenone were prepared at concentrations to have an absorbance of 0.3 at 266 nm (1 cm optical path length). The sample solutions were deoxygenated by argon purging.

High-performance liquid chromatography (HPLC) was performed on a system equipped with a photodiode array detector and an ESI mass detector. The injection volume was typical 10 μL. A reverse-phase C_{18} column (C_{18} 5 μm 4.6 × 100 mm column) was used for all HPLC runs. HPLC-grade water and acetonitrile were used as mobile phases with either isocratic or gradient modes. The flow rate for all HPLC runs was 1 mL/min. The system was equilibrated with the mobile phases for at least 20 min before each run. The samples being injected were dissolved in acetonitrile if not specified.

Quantum yield measurement. Valerophenone with a quantum yield of **1** (loss of valerophenone in acetonitrile solutions)[14] was used as actinometer for quantum yield measurements. The loss of valerophenone was quantified

dx.doi.org/10.1021/jo302149u | J. Org. Chem. 2013, 78, 1735−1741

by gas chromatography (GC) equipped with a flame ionization detector and a capillary column (Cp-Sil 5 CB low bleed/MS, 0.05 mm × 25 m, 0.25 μm particle size). A calibration curve for each compound was generated with at least five points, and the linear range of the detector was determined. In a typical quantum yield measurement, the absorbances of sample and the standard in acetonitrile solutions were matched at the irradiation wavelength. Two milliliters of the sample or standard solution was deoxygenated (argon bubbling) and irradiated in sealed 1 × 1 cm Suprasil quartz cells under stirring with a magnetic stirring bar using a low-pressure Hg lamp emitting at 254 or 300 nm as light source. Aliquots of the solution (15 μL) at different irradiation times were withdrawn from the photolysis cell for GC and HPLC analysis and quantified by calibration curves for each compound being analyzed. The conversions in these photoreactions were kept below 30% to minimize interference from secondary products.

■ ASSOCIATED CONTENT

Ⓢ Supporting Information

Additional HPLC traces, flash photolysis, and low-temperature phosphorescence results. This material is available free of charge via the Internet at http://pubs.acs.org.

■ AUTHOR INFORMATION

Corresponding Author

*E-mail: njt3@columbia.edu, willson@che.utexas.edu.

Notes

The authors declare no competing financial interest.

■ ACKNOWLEDGMENTS

The authors at Columbia thank the National Science Foundation for financial support through grant NSF-CHE-11-11398 and Intel Corporation for their support.

■ REFERENCES

(1) French, R. H.; Tran, H. V. *Annu. Rev. Mater. Res.* **2009**, *39*, 93−126.
(2) Gu, X.; Bates, C.; Cho, Y.; Coster, E.; Marzuka, F.; Nagai, T.; Ogata, T.; Shi, C.; Sundaresan, A. K.; Turro, N. J.; Bristol, R.; Zimmerman, P.; Willson, C. G. *J. Photopolym. Sci. Technol.* **2009**, *22*, 773−781.
(3) Gu, X.; Cho, Y.; Kawakami, T.; Hagiwara, Y.; Rawlings, B.; Mesch, R.; Ogata, T.; Kim, T.; Seshimo, T.; Wang, W.; Sundaresan, A. K.; Turro, N. J.; Gronheid, R.; Blackwell, J.; Bristol, R.; Willson, C. G. *Proc. SPIE* **2011**, *7972*, 79720F.
(4) Hagiwara, Y.; Mesch, R. A.; Kawakami, T.; Okazaki, M.; Jockusch, S.; Li, Y.; Turro, N. J.; Willson, C. G. *J. Org. Chem.* **2012**, DOI: 10.1021/jo3021488.
(5) Wagner, P. J. *Acc. Chem. Res.* **1971**, *4*, 168−177.
(6) Lalevee, J.; Allonas, X.; Fouassier, J. P.; Tachi, H.; Izumitani, A.; Shirai, M.; Tsunooka, M. *J. Photochem. Photobiol. A* **2002**, *151*, 27−37.
(7) Mallavia, R.; Sastre, R.; Amat-Guerri, F. *J. Photochem. Photobiol. A* **2001**, *138*, 193−201.
(8) Montalti, M.; Credi, A.; Prodi, L.; Gandolfi, M. T. *Handbook of Photochemistry*, 3rd ed.; CRC Press LLC: Boca Raton, FL, 2006.
(9) Schuster, D. I.; Dunn, D. A.; Heibel, G. E.; Brown, P. B.; Rao, J. M.; Woning, J.; Bonneau, R. *J. Am. Chem. Soc.* **1991**, *113*, 6245−6255.
(10) Wagner, P. J.; Klan, P. *J. Am. Chem. Soc.* **1999**, *121*, 9626−9636.
(11) McGarry, P. F.; Doubleday, C. E., Jr.; Wu, C.-H.; Staab, H. A.; Turro, N. J. *J. Photochem. Photobiol. A* **1994**, *77*, 109−117.
(12) Carmichael, I.; Helman, W. P.; Hug, G. L. *J. Phys. Chem. Ref. Data* **1987**, *16*, 239−260.
(13) Wagner, P. J.; May, M. J.; Haug, A.; Graber, D. R. *J. Am. Chem. Soc.* **1970**, *92*, 5269−5270.
(14) Wagner, P. J. *J. Am. Chem. Soc.* **1967**, *89*, 5898−5901.
(15) Wagner, P. J.; Kemppainen, A. E.; Schott, H. N. *J. Am. Chem. Soc.* **1973**, *95*, 5604−5614.
(16) Yagci, Y.; Jockusch, S.; Turro, N. J. *Macromolecules* **2007**, *40*, 4481−4485.